Galaxy Zoo: The interplay of quenching mechanisms in the group environment

R. J. Smethurst,[1] C. J. Lintott,[1] and the Galaxy Zoo team *

[1] *Oxford Astrophysics, Department of Physics, University of Oxford, Denys Wilkinson Building, Keble Road, Oxford, OX1 3RH, UK*

28 September 2016

ABSTRACT

Does the environment of a galaxy directly influence the quenching history of a galaxy? Here we construct a sample of group and field galaxies with morphological classifications from Galaxy Zoo 2 and use Bayesian inference to determine the quenching time and exponential timescale that describes a simple SFH for a given galaxy from its photometry. We observe how the detailed morphological structures, such as bars and bulges, are affected by the group environment and correlate this with changes in the quenching history. We find that the environment does play a direct role in galaxy quenching through a mechanism which is correlated to the halo mass of a group but not to the relative velocity of a satellite galaxy to its central. Environmental quenching mechanisms which are correlated with satellite velocity, such as ram pressure stripping, are not the main cause of quenching in the group environment. Instead an interplay of merger, mass, morphology and environmental quenching mechanisms dependent on the group potential drive the evolution of group galaxies.

Key words: galaxies – environment, galaxies – photometry, galaxies – statistics, galaxies – morphology

1 INTRODUCTION

There are many mechanisms which are proposed to cause quenching; including mergers (Daddi et al. 2010; Darg et al. 2010a; Cheung et al. 2012; Barro et al. 2013; Pontzen et al. 2016), AGN feedback (Di Matteo et al. 2005; Nandra et al. 2007), mass quenching (Peng et al. 2012), morphological quenching (Fang et al. 2013) and the environment of a galaxy (see review of mechanisms in Boselli & Gavazzi 2006, and references therein).

The galaxy environment as a cause of quenching was proposed due to the correlation of morphology (Dressler 1980; Smail et al. 1997; Poggianti et al. 1999; Postman et al. 2005; Bamford et al. 2009), star formation rate (SFR) and the quenched galaxy fraction (Kauffmann et al. 2003; Baldry et al. 2006; Peng et al. 2012; Darvish et al. 2016) with environmental density. However, do these correlations truly imply causation? Recent evidence from simulations suggests that the environment may not be the dominant quenching mechanism in the galaxy lifecycle. Perhaps instead, the correlation of increased galaxy quenched fractions with environment is due to a superposition of the effects of mergers & interactions and both mass & morphology quenching.

1.1 Mergers as a quenching mechanism

In denser environments, galaxies are more likely to encounter another galaxy in a merger or interaction scenario than when isolated in the field environment. When two galaxies merge, the influx of cold gas funnelled by the forces in the interaction often result in energetic starbursts and the fuelling of a central AGN (Hopkins et al. 2005), both of which can exhaust (and in the case of the AGN possibly expel) the gas required for star formation, effectively quenching the post-merger remnant galaxy (Pontzen et al. 2016).

1.2 Mass quenching

Mass quenching is the process by which a galaxy, independent of its environment, uses up its available gas for star formation via the Kennicutt-Schmidt law (Schmidt 1959; Kennicutt 1998) and consequently grows in mass. This is thought to be the dominant mechanism for isolated galaxies in the field (Kormendy & Kennicutt 2004). In groups and cluster environments, infall into the group can occur over long timescales during which gas reservoirs can be depleted via this mass quenching process.

1.3   Morphological quenching

Morphological quenching (or secular quenching) is the process by which the internal structure of a galaxy can impact on its SFR. This is theorised to occur in galaxies hosting bars; the bar funnels gas to the centre of the galaxy (Athanassoula 1992a) where it is exhausted by star formation effectively quenching the galaxy (Sheth et al. 2005; Zurita et al. 2004; Masters et al. 2010). Such a process has been postulated to be caused also by bulges (Bluck et al. 2014) and spiral (Hart et al. 2016) structures in galaxies.

1.4   Environmental quenching

The mechanisms under the umbrella of environmental quenching are numerous and varied. Together with the typical gravitational galaxy-galaxy interactions (Moore et al. 1996), environmental quenching also encapsulates hydrodynamic interactions occurring between the cold inter stellar medium (ISM) of the in-falling galaxy and the hot intergalactic medium (IGM) of the group or cluster. This includes such processes as ram pressure stripping (Gunn & Gott 1972), viscous stripping (Nulsen 1982), and thermal evaporation (a rapid rise in temperature of the ISM due to contact with the IGM; Cowie & Songaila 1977). Starvation (Larson et al. 1980) can remove the outer galaxy halo cutting off the star formation gas supply to a galaxy and preprocessing occurs when all of the above mechanisms take place in a group of galaxies which then falls into a larger cluster (Dressler 2004).

The most likely candidate (and therefore the most studied) mechanism for the cause of the environmental density-morphology and SFR relations is ram pressure stripping (RPS; Abadi et al. 1999; Poggianti et al. 1999). However, there has been mounting evidence that RPS may not be as effective as a quenching mechanism as first thought (Emerick et al. 2016; Fillingham et al. 2016).

1.5   Aims of this work

In order to isolate the case of the density-morphology and density-SFR correlations, we need to study how galaxy quenching timescales and morphology change in group and field environments with different properties. We use the group environment to study this problem, as this is a more typical environment for a galaxy than the relatively rare rich cluster environment (Carlberg 2004). To do this we construct a sample of both group and field galaxies and utilise Bayesian inference to determine the quenching time and exponential timescale to describe a simple SFH for a galaxy given its photometry. We aim to determine the following: (i) How does the environment influence the detailed morphological structures of a galaxy? (ii) Is environmental quenching occurring in the group environment?

In Section 2 we describe our data sources and inference methods and highlight our results in Section 3. We then discuss these results and how they fit into the bigger picture of quenching in Section 4. The zero points of all magnitudes are in the AB system. Where necessary, we adopt the WMAP Seven-Year Cosmology (Jarosik et al. 2011) with $(\Omega_m, \Omega_\Lambda, h) = (0.26, 0.73, 0.71)$.

2   DATA AND METHODS

2.1   Data Sources

In this investigation we use visual classifications of galaxy morphologies from the Galaxy Zoo 2[1] (GZ2) citizen science project (Willett et al. 2013), which obtains multiple independent classifications for each optical image. The full question tree for an image is shown in Figure 1 of Willett et al. The GZ2 project used $304,022$ images from the Sloan Digital Sky Survey Data Release 7 (SDSS; York et al. 2000; Abazajian et al. 2009) all classified by *at least* 17 independent users, with a mean number of classifications of ~ 42.

Further to this, we required NUV photometry from the GALEX survey (Martin et al. 2005), within which $\sim 42\%$ of the GZ2 sample was observed, giving $126,316$ galaxies total $(0.01 < z < 0.25)$. This will be referred to as the GZ2-GALEX sample. The completeness of this sample $(-22 < M_u < -15)$ is shown in Figure 2 of Smethurst et al. (2015).

Observed fluxes are corrected for galactic extinction (Oh et al. 2011) by applying the Cardelli et al. (1989) law. We also adopt k-corrections to $z = 0.0$ and obtain absolute magnitudes from the NYU-VAGC (Blanton et al. 2005; Blanton & Roweis 2007; Padmanabhan et al. 2008).

2.1.1   Group Identification

We used the Berlind et al. (2006) catalogue, which uses a friends-of-friends algorithm to identify group and cluster galaxies in the SDSS. This was cross matched to the GZ2-GALEX sample and limited to $z < 0.1$ to ensure GALEX completeness of the red sequence (see Wyder et al. 2007; Yesuf et al. 2014). Centrals were selected as the most massive galaxy in a group and all others were designated as satellites (masses were calculated using the absolute r-band magnitude and $u - r$ colour and the method of Baldry et al. 2006). The projected cluster centric radius, R, of all satellite galaxies was calculated from the projected separations of a satellite from its central (converted to kpc from a consideration of the observed redshift of the central galaxy) which was then normalised by the R_{200} of the group (the radius within which the mass overdensity is 200 times the critical density; see Finn et al. 2005), often used as a proxy for the virial radius of the group (Navarro et al. 1995). This resulted in a sample of $14,199$ group galaxies with $3,468$ centrals and $10,731$ satellites within a projected cluster centric radius range of $0 < R/R_{200} < 25$ and $z < 0.084$.

In this work we focus on galaxies which are either quenching or quenched and are more than $\pm 1\sigma$ below the star forming 'main sequence'. This encompasses 4629 satellite and 2314 central galaxies and will be referred to as the GZ2-GROUP sample. These galaxies are highlighted in the panels of Figure 2.1 and can be seen to lie below the 'main sequence' of star formation.

We obtain masses and velocity dispersions of galaxies in the GZ2-GROUP sample from the MPA-JHU catalogue (Kauffmann et al. 2003; Brinchmann et al. 2004).

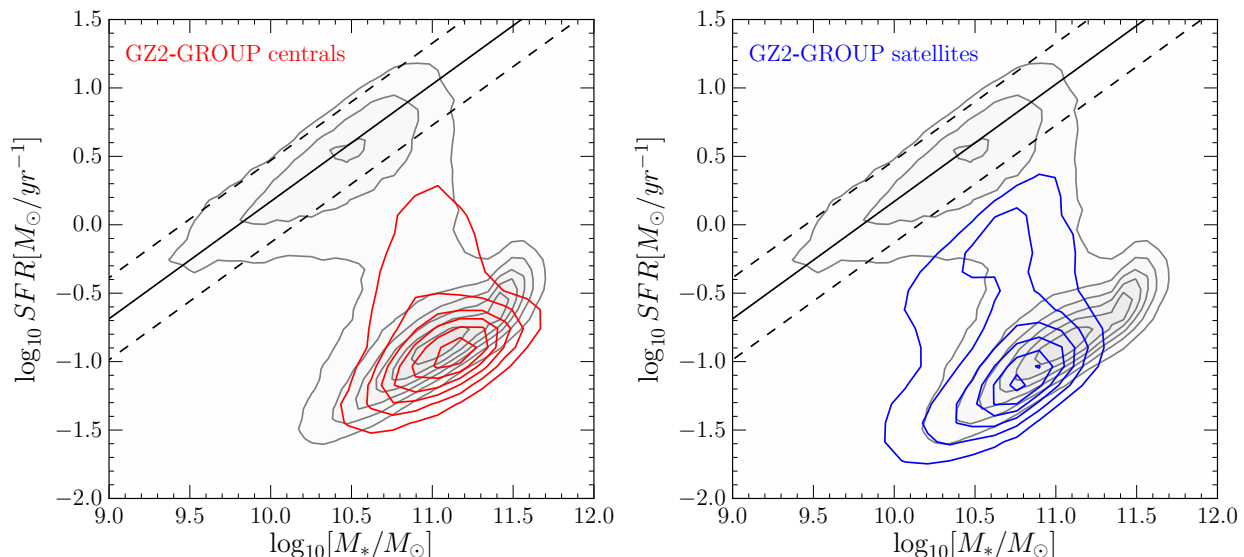[1] http://zoo2.galaxyzoo.org/

Figure 1. The SFR-stellar mass plane showing central (left; red contours) and satellite (right; blue contours) galaxies in the GZ2-GROUP sample. In both panels the entire SDSS sample from the MPA-JHU catalog is shown by the grey filled contours. The definition of the star forming "main sequence" from Peng et al. (2010) at $\overline{z} = 0.083$ (solid line, the mean redshift of the AGN-HOST sample) with $\pm 1\sigma$ (dashed lines) is shown.

2.1.2 Field sample

For all galaxies in the GZ2-GALEX sample, we calculated the smallest projected cluster centric radii, R/R_{200}, from each of the central galaxies in the Berlind et al. (2006) catalog and selected candidate field galaxies as those with (i) $R/R_{200} > 25$ and (ii) $\log \Sigma < -0.8$ (a measure of environmental density from Baldry et al. 2006). This sample of field galaxy candidates was then matched in redshift and stellar mass firstly to the central galaxies of the GZ2-GROUP sample to give $2,309$ field galaxies with $z < 0.084$ which will be referred to as the GZ2-CENT-FIELD sample. In this work we focus on galaxies which are either quenching or quenched and are more than $\pm 1\sigma$ below the star forming 'main sequence'. This encompasses $1,596$ field galaxies with $z < 0.084$ which will be referred to as the GZ2-CENT-FIELD-Q sample and used as a control sample when investigating the trends with central galaxy properties of the inferred quenching parameters.

The redshift distribution of the GZ2-CENT-FIELD-Q sample is shown in comparison to the distribution of central galaxies in the GZ-GROUP sample in Figure 2.1.2.

Secondly, the field galaxy candidates were then matched in redshift and stellar mass to the satellite galaxies of the GZ2-GROUP sample to give $6,849$ field galaxies with $z < 0.084$ which will be referred to as the GZ2-SAT-FIELD. These galaxies in the GZ2-SAT-FIELD sample will be used as a control when investigating the morphological trends of satellite galaxies with environment. Note that the sample is not restricted to being $\pm 1\sigma$ below the star forming 'main sequence' in this case.

We obtain masses, SFRs and velocity dispersions of galaxies for all of the field samples described above from the MPA-JHU catalogue (Kauffmann et al. 2003; Brinchmann et al. 2004).
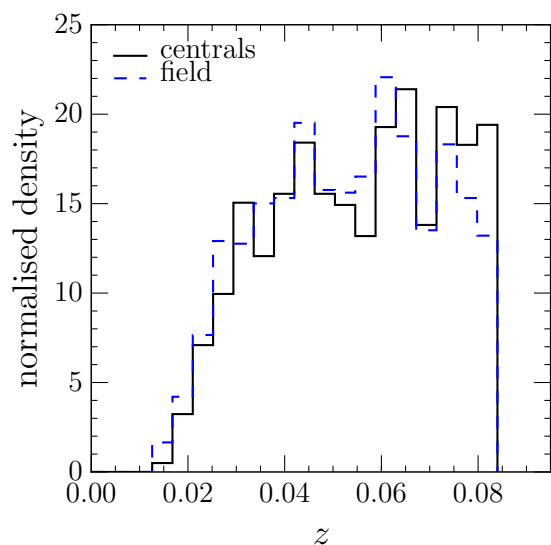

Figure 2. Redshift distributions of central galaxies in the GZ2-GROUP sample (black solid line) in comparison to the redshift and mass matched GZ2-CENT-FIELD-Q sample (blue dashed line).

2.2 Deriving quenching parameters

STARPY[2] is a PYTHON code which allows the user to derive the quenching star formation history (SFH) of a single galaxy through a Bayesian Markov Chain Monte Carlo method (Foreman-Mackey et al. 2013)[3] with the input of

---

[2] Publicly available: `http://github.com/zooniverse/starpy`
[3] `http://dan.iel.fm/emcee/`

the observed $u - r$ and $NUV - u$ colours, a redshift, and the use of the stellar population models of Bruzual & Charlot (2003). These models are implemented using solar metallicity (varying this does not substantially affect these results; Smethurst et al. 2015) and a Chabrier IMF (Chabrier 2003) but does not model for intrinsic dust. The SFH is modelled as an exponential decline of the SFR described by two parameters $[t_q, \tau]$, where t_q is the time at the onset of quenching [Gyr] and τ is the exponential rate at which quenching occurs [Gyr]. Under the simplifying assumption that all galaxies formed at $t = 0$ Gyr with an initial burst of star formation, the SFH can be described as:

$$SFR = \begin{cases} i_{sfr}(t_q) & \text{if } t < t_q \\ i_{sfr}(t_q) \times exp\left(\frac{-(t-t_q)}{\tau}\right) & \text{if } t > t_q \end{cases} \quad (1)$$

where i_{sfr} is an initial constant star formation rate (SFR) dependent on t_q (Schawinski et al. 2014; Smethurst et al. 2015). A smaller τ value corresponds to a rapid quench, whereas a larger τ value corresponds to a slower quench. We note that a galaxy undergoing a slow quench is not necessarily quiescent by the time of observation. Similarly, despite a rapid quenching rate, star formation in a galaxy may still be ongoing at very low rates, rather than being fully quenched. This SFH model has previously been shown to appropriately characterise quenching galaxies (Weiner et al. 2006; Martin et al. 2007; Noeske et al. 2007; Schawinski et al. 2014). We note also that star forming galaxies in this regime are fit by a constant SFR with a $t_q \simeq \text{Age}(z)$, (i.e. the age of the Universe at the galaxy's observed redshift) with a very low probability.

The probabilistic fitting methods to these star formation histories for an observed galaxy are described in full detail in Section 3.2 of Smethurst et al. (2015), wherein the STARPY code was used to characterise the SFHs of each galaxy in the GZ2-GALEX sample. We assume a flat prior on all the model parameters and the difference between the observed and predicted $u - r$ and $NUV - u$ colours are modelled as independent realisations of a double Gaussian likelihood function (Equation 2 in Smethurst et al. 2015). We also make the simplifying assumption that the age of each galaxy, t_{age} corresponds to the age of the Universe at its observed redshift, t_{obs}.

We note also that galaxy colours were not corrected for intrinsic dust attenuation. This is of particular consequence for disc galaxies, where attenuation increases with increasing inclination. Buat et al. (2005) found the median value of the attenuation in the GALEX NUV passband to be ~ 1 mag. Similarly Masters et al. (2010) found a total extinction from face-on to edge-on spirals of 0.7 and 0.5 mag for the SDSS u and r passbands and show spirals with $\log(a/b) > 0.7$ have signs of significant dust attenuation. However, we showed from an investigation into this problem in Section 2.2 of Smethurst et al. (2016) that internal galactic extinction does not systematically bias our results from STARPY.

The output of STARPY is probabilistic in nature and provides the posterior probability distribution across the two-parameter space for an individual galaxy the degeneracies for which can be seen in Figure 4 of Smethurst et al. (2015). Whereas in previous studies that distributions have been weight and combined to give an overall distribution representing the population of galaxies (see Smethurst et al. 2015,
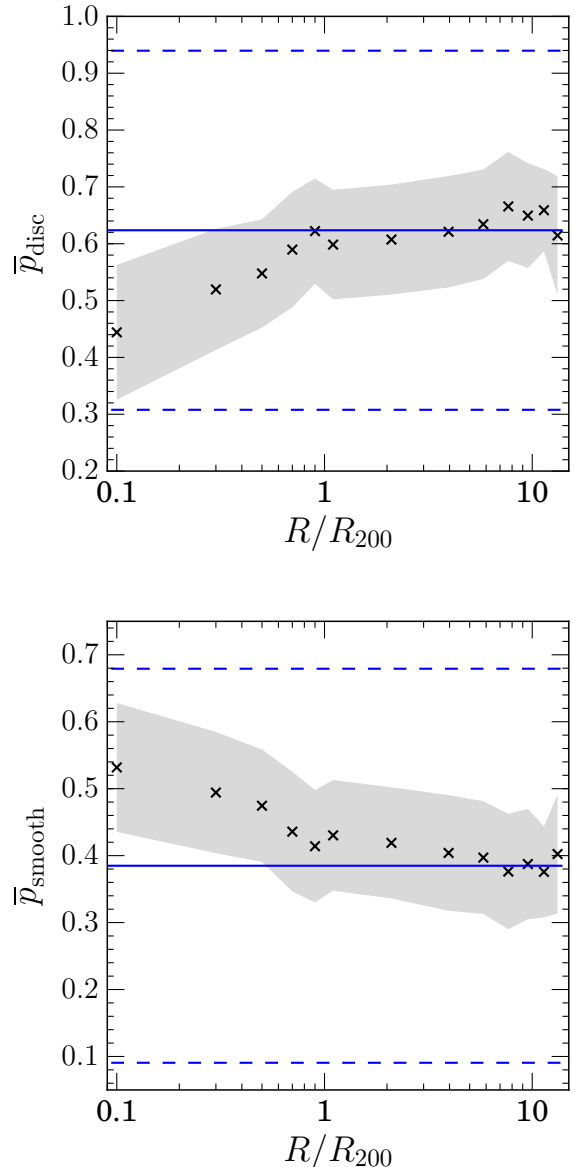

Figure 3. Mean GZ vote fraction for disc (top) and smooth (bottom) galaxies in the GZ2-GROUP sample binned in projected cluster centric radius, normalised by R_{200}, a proxy for the virial radius of a group. The shaded region shows $\pm 1\sigma$ on the mean vote fraction. The mean vote fraction of the GZ2-SAT-FIELD sample are also shown (blue solid lines) with $\pm 1\sigma$ (blue dashed lines).

2016), due to the complex nature of the group environment here we choose instead to take the 50th percentile walker position of these individual posterior probability distributions to give the most likely t_q and τ for each galaxy.

This simplifies the output from STARPY for each galaxy from a probability distribution to two more manageable values. In this work we will look for trends in the time since quenching onset, Δt, for a given galaxy by calculating $\Delta t = t_{obs} - t_q$. We will observe how this quantity changes with group properties, including halo mass (here we use the stellar mass of the group central as a proxy for halo mass),
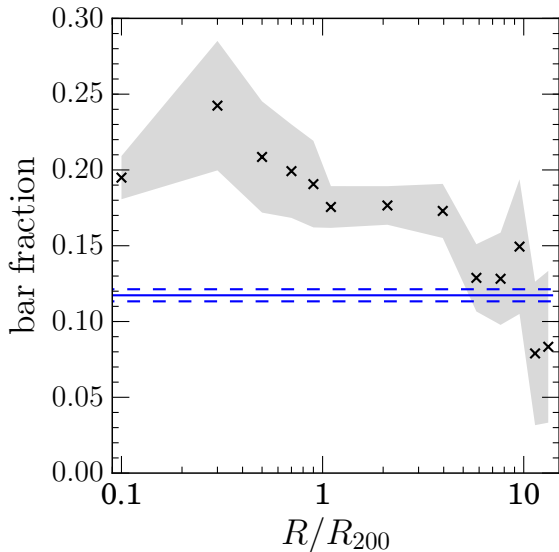
Figure 4. Bar fraction (number of barred disc galaxies over number of disc galaxies) in the GZ2-GROUP sample binned in projected cluster centric radius, normalised by R_{200}, a proxy for the virial radius of a group. The shaded region shows $\pm 1\sigma$ on the bar fraction. The bar fraction of the GZ2-SAT-FIELD sample is also shown (blue solid line) with $\pm 1\sigma$ (blue dashed line).

velocity dispersion, number of group members and relative velocity of a satellite galaxy.

3 RESULTS

3.1 Dependence of detailed morphological structure with environment

Figure 3 shows the mean disc and smooth vote fractions from GZ2, binned in projected cluster centric radius (normalised by the approximate viral radius of each group, R_{200}). We can see that the mean disc (smooth) vote fraction decreases (increases) from the mean field value (blue line) under 1 virial radius, in agreement with previous studies on the morphology-density relation (Dressler 1980; Smail et al. 1997; Poggianti et al. 1999; Postman et al. 2005; Bamford et al. 2009). Along with this initial sanity check on the GZ2-GROUP sample, the extensive morphological classifications provided by GZ2 allows us to now investigate how more detailed morphological structure is affected by the group environment.

Figure 4 shows how the bar fraction (number of barred disc galaxies over the number of disc galaxies) increases towards the centre of the group population, significantly over the field fraction (blue solid line). Figure 5 shows how the merger fraction does not significantly deviate from the field fraction (blue solid line) until within $\sim$ virial radius. Similarly, the left panel of Figure 6 shows how those galaxies identified as having no or just noticeable bulges are less common in the inner regions of the cluster (left panel), whereas the fraction of galaxies with obvious or dominant bulges increases with decreasing projected distance from the centre of the cluster.
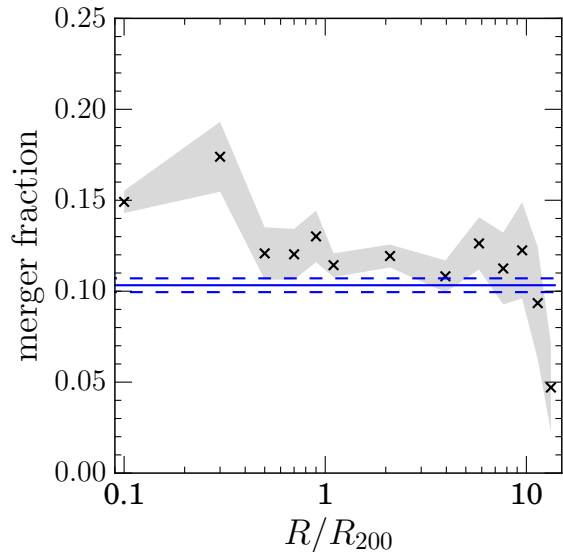
Figure 5. Merger fraction in the GZ2-GROUP sample binned in projected cluster centric radius, normalised by R_{200}, a proxy for the virial radius of a group. The shaded region shows $\pm 1\sigma$ on the merger fraction. The merger fraction of the GZ2-SAT-FIELD sample is also shown (blue solid line) with $\pm 1\sigma$ (blue dashed line).

3.2 Quenching times in the group environment

With the output from STARPY we can also study the time since quenching onset ($\Delta t = t_{obs} - t_q$, see Section 2.2) binned in projected cluster centric radius, normalised by R_{200} (a proxy for virial radius) for satellite galaxies and central galaxies in the GZ2-GROUP sample, compared with galaxies in the GZ2-FIELD sample. This is shown in Figures 7 & 8 and we investigate trends in Δt by binning by various group properties:

• Stellar mass, M_*: in the top panel of Figure 7 galaxies in the GZ2-GROUP sample are now split by their stellar mass and we see a clear trend for increasing time since quenching onset with increasing stellar mass for satellite, central and field galaxies. The central galaxies (shown by the square points at $\sim 0.01 R/R_{200}$) appear to have quenched more recently than the inner satellites (at $\sim 0.1 R/R_{200}$) of the same mass.

• Halo mass: in the middle panel of Figure 7 we use a proxy for halo mass by splitting by the GZ2-GROUP sample by the stellar mass of the corresponding central galaxy of a group, $M_{c,*}$ and find a clear trend for increasing time since quenching onset with increasing stellar mass of the group central for satellite, central and field galaxies.

• Mass ratio, $\mu_* = M_*/M_{*,c}$: the stellar mass ratio of the satellite to its central galaxy. In the bottom panel of Figure 7 we show the time since quenching of the GZ2-GROUP split into bins of $\log_{10} \mu_*$. The change in Δt with projected cluster centric radius occurs more steeply (particularly beyond $\sim$ a virial radius) for satellite galaxies with much smaller masses than their group central ($-2.0 < \log_{10} \mu_* < -1.0$, shown by the blue curve).

• Number of group members, N_{group}: the top panel of Figure 8 shows that there is no trend with time since
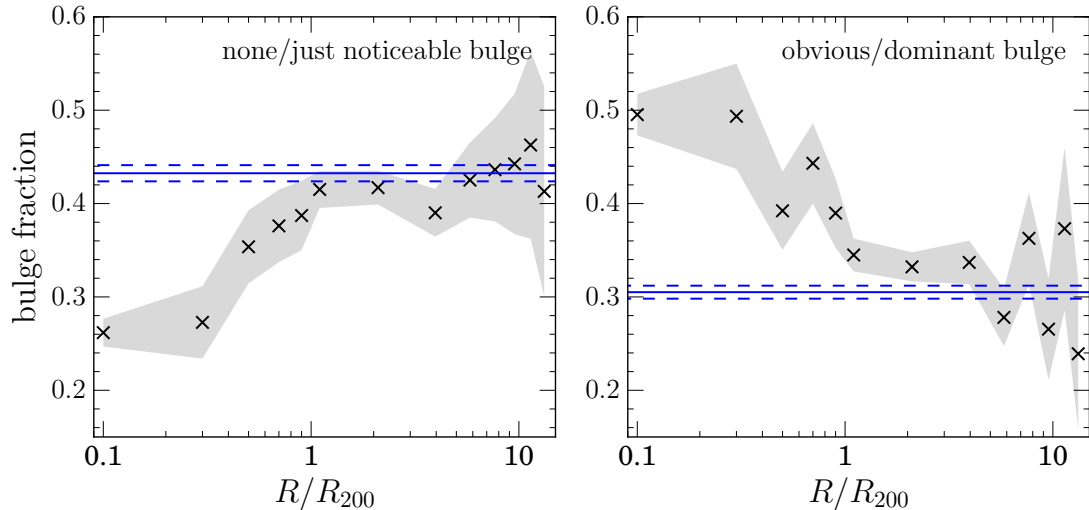
Figure 6. Fraction of galaxies with none/just noticeable bulge classifications (left) and with obvious/dominant bulge classifications (right) in the GZ2-GROUP sample binned in projected cluster centric radius, normalised by R_{200}, a proxy for the virial radius of a group. The shaded regions shows $\pm1\sigma$ on the bulge fractions. The bulge fractions of the GZ2-SAT-FIELD sample are also shown (blue solid lines) with $\pm1\sigma$ (blue dashed lines).

quenching onset with increasing N_{group} for satellite galaxies. The central galaxies (shown by the square points at $\sim 0.01R/R_{200}$) however, do show a trend for increasing time since quenching with N_group.

• Relative velocity, $|\Delta v|$: in the bottom panel of Figure 8 we split the satellite galaxies of the GZ2-GROUP sample into bins of relative velocity to their central galaxies. We can see that there is no trend with time since onset of quenching with increasing relative velocity for galaxies in the group environment.

• Stellar velocity dispersion, σ_*: the bottom panel of Figure 8 shows the time since quenching of the GZ2-GROUP sample split into bins of σ_*. The stellar velocity dispersion shows the largest trend in Δt for satellite galaxies of all of the group properties studied, with galaxies with the smallest (largest) stellar velocity dispersions have quenched more (less) recently.

Across all the panels in Figures 7 & 8 we see a general trend for increasing time since quenching onset with decreasing distance from the group centre. As earlier, in Figures 3−6 significant differences from the field value arise inside $\sim$ one virial radius.

4   DISCUSSION

4.1   The role of mergers in quenching in the group environment

The merger classification in GZ2 has been shown to preferentially identify major mergers (Darg et al. 2010b). Similarly, bulge formation in disc galaxies is often associated with (minor) merger driven evolutionary histories (Croton et al. 2006; Tonini et al. 2016). Although we see evidence for an enhanced merger fraction in the inner regions of the group environment in Figure 5, the bulge fractions in Figure

6 vary much more significantly from the field value than the merger fraction. This suggests that minor mergers may be more dominant than major mergers in the group environment, particularly at $R/R_{200} > 0.5$.

If mergers are an important evolutionary mechanism for satellite galaxies, as the morphological evidence in Figures 5 & 6 suggests, we would expect to see a difference in the quenching histories of satellites residing in groups with a larger number of members. However, the top panel of Figure 8 shows there is no trend with time since quenching onset with increasing N_{group} for the satellite galaxies. This suggests that mergers are not the dominant quenching mechanism for satellite galaxies.

For central galaxies however, this is not the case. The central galaxies (shown by the square points at $\sim 0.01R/R_{200}$ in the top panel of Figure 8), do show a trend for increasing time since quenching with increasing N_{group}. Therefore, we can postulate that the larger the number of group members, the more important mergers are for a central's evolutionary history.

This idea is supported by the result shown in the top panel of Figure 7 when the GZ2-GROUP is split into bins of stellar mass. We can see that centrals of a given mass have quenched more recently than the inner satellites (at $\sim 0.1R/R_{200}$) of a given mass. This suggests that an episode of more recent star formation may have occurred in the central galaxies but not in the inner satellites. This is once again suggestive of a merger dominated evolutionary history for central galaxies, as mergers are thought to cause an energetic burst of star formation which in turn quenches the remnant galaxy (Hopkins et al. 2005; Treister et al. 2012; Pontzen et al. 2016). If the central galaxies have quenched more recently than the inner satellites this could be a more recent burst of star formation caused by a merger under this regime.
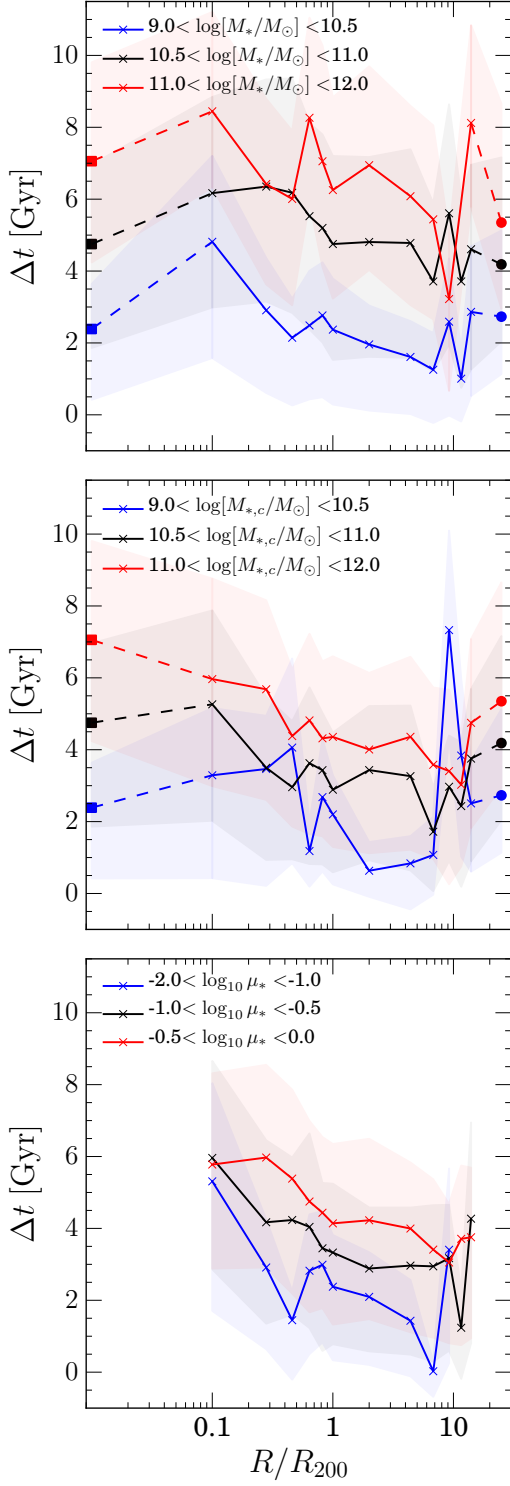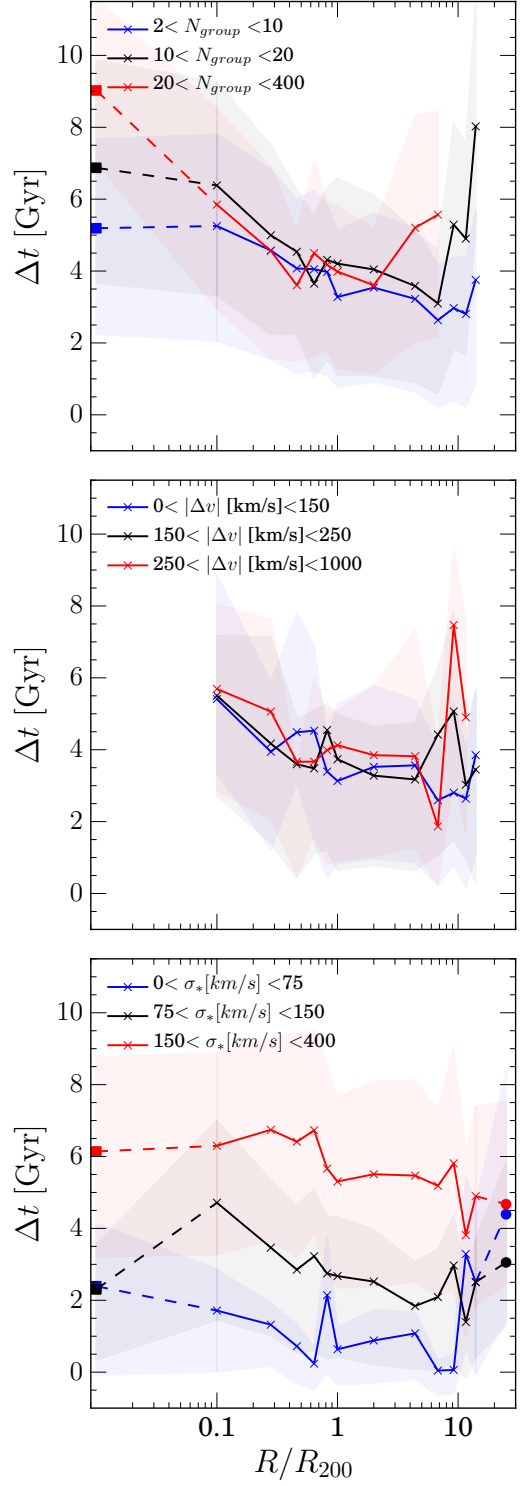
Figure 7. The time since quenching onset ($\Delta t = t_{obs} - t_q$) binned in projected cluster centric radius, normalised by R_{200}, for satellite galaxies (crosses) split into bins of stellar mass (top), stellar mass of the corresponding central galaxy (middle; a proxy for halo mass of a group) and the stellar mass ratio ($\mu_* = M_*/M_{*,c}$, bottom). The corresponding values for central galaxies (squares, plotted at $0.01R/R_{200}$) and galaxies in the GZ2-CENT-FIELD-Q sample (circles, plotted at $25R/R_{200}$) are shown where calculable and connected by the dashed lines to help guide the eye. The shaded regions show the $\pm 1\sigma$ on Δt in each bin of R/R_{200}.

Figure 8. The time since quenching onset ($\Delta t = t_{obs} - t_q$) binned in projected cluster centric radius, normalised by R_{200}, for satellite galaxies (crosses) split by the number of group members (N_{group}, top), absolute relative velocity of the satellite to its central galaxy ($|\Delta v|$, middle) and velocity dispersion (σ_*, bottom). The corresponding values for central galaxies (squares, plotted at $0.01R/R_{200}$) and galaxies in the GZ2-CENT-FIELD-Q sample (circles, plotted at $25R/R_{200}$) are shown where calculable and connected to the satellite values by the dashed lines to help guide the eye. The shaded regions show the $\pm 1\sigma$ on Δt in each bin of R/R_{200}.

4.2   The role of mass quenching in the group environment

The role of mass quenching in the group environment is apparent in the top panel of Figure 7 and the bottom panel of Figure 8 where the GZ2-GROUP satellites are binned by stellar mass and central velocity dispersions respectively. We see a trend for increasing time since quenching with increasing stellar mass and velocity dispersion for centrals, satellites and field galaxies. This is suggestive of mass quenching occurring across the entire galaxy population irrespective of environmental density, supporting the work of Peng et al. (2010); Gabor et al. (2010); Peng et al. (2012) and Darvish et al. (2016).

4.3   The role of morphological quenching in the group environment

The results in Figure 4, showing the increasing bar fraction towards the central group regions which is consistent with results that show that bars themselves may be the cause of morphological quenching through the funnelling of gas toward the central regions of galaxies (Athanassoula 1992b; Sheth et al. 2005; Masters et al. 2010). However we must consider whether the environment itself may play a role in triggering the disk instabilities which can produce a morphological bar. Indeed harassment and tidal interactions have been shown to both promote and inhibit bar formation dependent on the stellar mass (Noguchi 1988; Moore et al. 1996; Skibba et al. 2012). In this case, morphological quenching would be occurring but indirectly due to environmental quenching.

4.4   The role of the environment in quenching

Across all panels of Figures 7-8 a trend for increasing time since quenching onset with decreasing projected cluster centric radius is present. This suggests that the environment does directly cause quenching throughout the infall time of a galaxy in a group. Those galaxies closer in, fell into the group earlier and as they did so they started to quench, giving rise to a larger inferred Δt.

In the top panel of Figure 7 we also see a clear trend for increasing Δt with increasing stellar mass of the group central for both satellite and central galaxies. More massive halos therefore have a greater impact on the star formation histories of their satellites than less massive halos. If we account for both the stellar mass and the halo mass of the central galaxy simultaneously by considering the stellar mass ratio of the satellite to its central galaxy, $\mu_* = M_*/M_{*,c}$ (see the bottom panel of Figure 7) we see that the change in Δt with projected cluster centric radius occurs more steeply (particularly at $R/R_{200} \lesssim 1$) for satellite galaxies with much smaller masses than their group central. The stellar mass of the central galaxy is used as a proxy for halo mass which is correlated with both (i) the gravitational potential of the group and (ii) the temperature of the IGM.

It is thought that higher mass halos have hotter inter galactic medium (IGM) temperatures which can then have a greater impact impact on a galaxy through RPS of cold gas. If RPS is indeed a dominant environmental quenching mechanism we should see a trend in Δt with the speed of a satellite galaxy relative to the group central. However in the middle panel of Figure 8 we see that this is not the case.

This suggests that any environmental quenching mechanism responsible for the trends seen in Δt with the mass of the corresponding central galaxy and mass ratio of the satellite to its central (middle and bottom panels of Figure 7 respectively) are not corrected with satellite velocity. This therefore rules out RPS as the dominant environmental quenching mechanism, in support of the conclusions of Emerick et al. (2016); Fillingham et al. (2016). The dominant environmental quenching mechanism in the group environment must therefore be correlated with the group potential. This suggests that satellite galaxies may be most affected by gravitationally driven environmental effects, such as harassment and galaxy-galaxy interactions or by thermal evaporation of the galaxy halo due to the hot IGM.

4.5   The Big Picture

In the previous sections we have discussed how our results of the changing morphological features and quenching times with projected cluster centric radius in the group and field environments show evidence for both merger, mass, morphological and environmentally driven evolutionary histories. This suggests that not one mechanism is dominant in the group environment but that a superposition of all these effects gives rise to the observed morphology-density and morphology-SFR relations.

Just as galaxy morphology is a spectrum from disc-dominated to spheroid-dominated systems, so too are the quenching mechanisms which cause this morphological transformation. Mergers and interactions are a spectrum of mass ratios from micro mergers (Carlin et al. 2016) through to major mergers, which have increasingly devastating impact upon the morphology and SFR of a galaxy. Morphological quenching mechanisms lie on a spectrum of stellar mass, and have a larger impact on those galaxies with smaller masses. Environmental quenching mechanisms lie on a spectrum of increasing group potential, giving rise to a stronger impact on the SFR of smaller mass galaxies in larger halos.

All of these mechanisms are striving towards the same end result with no single mechanism dominating over the other, except in the most extreme of environments. Mechanisms traditionally associated with the field, such as mass & morphology quenching also occur in more dense environments, however will often (after a long infall to the central regions of a group) be overwhelmed by those more rapid and violent mechanisms of mergers and interactions (and the triggered outflows from AGN that are associated with such mechanisms; see Smethurst et al. 2016). Similarly, environmental quenching mechanisms caused by the dense halo and hot IGM are influential as soon as a galaxy falls into a group or cluster, but such processes can also be interrupted momentarily by an interaction or a merger as a galaxy traverses the more dense environment.

5   CONCLUSIONS

Mergers, mass quenching morphology quenching and environmental quenching are all prevalent in galaxy groups. The environment does play a role in quenching galaxies through

a mechanism proportional to the halo mass of the group but not proportional to the relative speed of the satellite galaxy to its central galaxy. This suggests that ram pressure stripping is not the dominant environmental quenching mechanism. All of these mechanisms discussed coalesce to give rise to the distributions in galaxy properties we see across the Universe through their constant interplay across cosmic time.

REFERENCES

Abadi M. G., Moore B., Bower R. G., 1999, MNRAS, 308, 947
Abazajian K. N. et al., 2009, ApJS, 182, 543
Astropy Collaboration et al., 2013, A&A, 558, A33
Athanassoula E., 1992a, MNRAS, 259, 328

---

[4] `http://www.astropy.org/`

Athanassoula E., 1992b, MNRAS, 259, 345
Baldry I. K., Balogh M. L., Bower R. G., Glazebrook K., Nichol R. C., Bamford S. P., Budavari T., 2006, MNRAS, 373, 469
Bamford S. P. et al., 2009, MNRAS, 393, 1324
Barro G. et al., 2013, ApJ, 765, 104
Berlind A. A. et al., 2006, ApJS, 167, 1
Blanton M. R., Eisenstein D., Hogg D. W., Schlegel D. J., Brinkmann J., 2005, ApJ, 629, 143
Blanton M. R., Roweis S., 2007, AJ, 133, 734
Bluck A. F. L., Mendel J. T., Ellison S. L., Moreno J., Simard L., Patton D. R., Starkenburg E., 2014, MNRAS, 441, 599
Boselli A., Gavazzi G., 2006, PASP, 118, 517
Brinchmann J., Charlot S., White S. D. M., Tremonti C., Kauffmann G., Heckman T., Brinkmann J., 2004, MNRAS, 351, 1151
Bruzual G., Charlot S., 2003, MNRAS, 344, 1000
Buat V. et al., 2005, ApJ, 619, L51
Cardelli J. A., Clayton G. C., Mathis J. S., 1989, ApJ, 345, 245
Carlberg R. G., 2004, Clusters of Galaxies: Probes of Cosmological Structure and Galaxy Evolution, 343
Carlin J. L., Beaton R. L., Martínez-Delgado D., Gabany R. J., 2016, in Astrophysics and Space Science Library, Vol. 420, Astrophysics and Space Science Library, Newberg H. J., Carlin J. L., eds., p. 219
Chabrier G., 2003, PASP, 115, 763
Cheung E. et al., 2012, ApJ, 760, 131
Cowie L. L., Songaila A., 1977, Nature, 266, 501
Croton D. J. et al., 2006, MNRAS, 365, 11
Daddi E. et al., 2010, ApJ, 714, L118
Darg D. W. et al., 2010a, MNRAS, 401, 1552
Darg D. W. et al., 2010b, MNRAS, 401, 1043
Darvish B., Mobasher B., Sobral D., Rettura A., Scoville N., Faisst A., Capak P., 2016, ApJ, 825, 113
Di Matteo T., Springel V., Hernquist L., 2005, Nature, 433, 604
Dressler A., 1980, ApJ, 236, 351
Dressler A., 2004, in IAU Colloq. 195: Outskirts of Galaxy Clusters: Intense Life in the Suburbs, Diaferio A., ed., pp. 341–346
Emerick A., Mac Low M.-M., Grcevich J., Gatto A., 2016, ApJ, 826, 148
Fang J. J., Faber S. M., Koo D. C., Dekel A., 2013, ApJ, 776, 63
Fillingham S. P., Cooper M. C., Pace A. B., Boylan-Kolchin M., Bullock J. S., Garrison-Kimmel S., Wheeler C., 2016, MNRAS
Finn R. A. et al., 2005, ApJ, 630, 206
Foreman-Mackey D., Hogg D. W., Lang D., Goodman J., 2013, PASP, 125, 306
Gabor J. M., Davé R., Finlator K., Oppenheimer B. D., 2010, MNRAS, 407, 749
Gunn J. E., Gott, III J. R., 1972, ApJ, 176, 1
Hart R. E. et al., 2016, MNRAS, 461, 3663
Hopkins P. F. et al., 2005, in Bulletin of the American Astronomical Society, Vol. 37, American Astronomical Society Meeting Abstracts, p. 1354
Jarosik N. et al., 2011, ApJS, 192, 14
Kauffmann G. et al., 2003, MNRAS, 346, 1055
Kennicutt, Jr. R. C., 1998, ApJ, 498, 541

Kormendy J., Kennicutt, Jr. R. C., 2004, ARA&A, 42, 603

Larson R. B., Tinsley B. M., Caldwell C. N., 1980, ApJ, 237, 692

Martin D. C. et al., 2005, ApJ, 619, L1

Martin D. C. et al., 2007, ApJS, 173, 342

Masters K. L. et al., 2010, MNRAS, 405, 783

Moore B., Katz N., Lake G., Dressler A., Oemler A., 1996, Nature, 379, 613616

Nandra K. et al., 2007, ApJ, 660, L11

Navarro J. F., Frenk C. S., White S. D. M., 1995, MNRAS, 275, 56

Noeske K. G. et al., 2007, ApJ, 660, L43

Noguchi M., 1988, A&A, 203, 259

Nulsen P. E. J., 1982, MNRAS, 198, 1007

Oh K., Sarzi M., Schawinski K., Yi S. K., 2011, ApJS, 195, 13

Padmanabhan N. et al., 2008, ApJ, 674, 1217

Peng C. Y., Ho L. C., Impey C. D., Rix H.-W., 2010, AJ, 139, 2097

Peng Y.-j., Lilly S. J., Renzini A., Carollo M., 2012, ApJ, 757, 4

Poggianti B. M., Smail I., Dressler A., Couch W. J., Barger A. J., Butcher H., Ellis R. S., Oemler, Jr. A., 1999, ApJ, 518, 576

Pontzen A., Tremmel M., Roth N., Peiris H. V., Saintonge A., Volonteri M., Quinn T., Governato F., 2016, ArXiv e-prints, 1607.02507

Postman M. et al., 2005, ApJ, 623, 721

Schawinski K. et al., 2014, MNRAS, 440, 889

Schmidt M., 1959, ApJ, 129, 243

Sheth K., Vogel S. N., Regan M. W., Thornley M. D., Teuben P. J., 2005, ApJ, 632, 217

Skibba R. A. et al., 2012, MNRAS, 423, 1485

Smail I., Dressler A., Couch W. J., Ellis R. S., Oemler, Jr. A., Butcher H., Sharples R. M., 1997, ApJS, 110, 213

Smethurst R. J. et al., 2016, MNRAS

Smethurst R. J. et al., 2015, MNRAS, 450, 435

Taylor M. B., 2005, in Astronomical Society of the Pacific Conference Series, Vol. 347, Astronomical Data Analysis Software and Systems XIV, Shopbell P., Britton M., Ebert R., eds., p. 29

Tonini C., Mutch S. J., Croton D. J., Wyithe J. S. B., 2016, MNRAS, 459, 4109

Treister E., Schawinski K., Urry C. M., Simmons B. D., 2012, ApJ, 758, L39

Weiner B. J. et al., 2006, ApJ, 653, 1049

Willett K. W. et al., 2013, MNRAS, 435, 2835

Wyder T. K. et al., 2007, ApJS, 173, 293

Yesuf H. M., Faber S. M., Trump J. R., Koo D. C., Fang J. J., Liu F. S., Wild V., Hayward C. C., 2014, ApJ, 792, 84

York D. G. et al., 2000, AJ, 120, 1579

Zurita A., Relaño M., Beckman J. E., Knapen J. H., 2004, A&A, 413, 73